

Article

An Electro-Thermal Analysis of a Variable-Speed Doubly-Fed Induction Generator in a Wind Turbine

Yingning Qiu ^{1,*}, Wenxiu Zhang ^{1,†}, Mengnan Cao ^{1,†}, Yanhui Feng ^{1,†} and David Infield ²

¹ School of Energy and Power Engineering, Nanjing University of Science and Technology, Nanjing 210094, China; E-Mails: imzhangwx@163.com (W.Z.); dl_cmn@sina.com (M.C.); yanhui.feng@njust.edu.cn (Y.F.)

² Department of Electronic and Electrical Engineering, Strathclyde University, Glasgow G1 1XQ, UK; E-Mail: david.infield@eee.strath.ac.uk

† These authors contributed equally to this work.

* Author to whom correspondence should be addressed; E-Mail: yingningqiu@yahoo.com or yingning.qiu@njust.edu.cn; Tel.: +86-25-8431-7344 (ext. 903); Fax: +86-25-8431-4960.

Academic Editor: Frede Blaabjerg

Received: 5 December 2014 / Accepted: 9 April 2015 / Published: 24 April 2015

Abstract: This paper focuses on the electro-thermal analysis of a doubly-fed induction generator (DFIG) in a wind turbine (WT) with gear transmission configuration. The study of the thermal mechanism plays an important role in the development of cost-effective fault diagnostic techniques, design for reliability and premature failure prevention. Starting from an analysis of the DFIG system control and its power losses mechanism, a model that synthesizes the thermal mechanism of the DFIG and a WT system principle is developed to study the thermodynamics of generator stator winding. The transient-state and steady-state temperature characteristics of stator winding under constant and step-cycle patterns of wind speed are studied to show an intrinsic thermal process within a variable-speed WT generator. Thermal behaviors of two failure modes, *i.e.*, generator ventilation system failure and generator stator winding under electric voltage unbalance, are examined in details and validated by both simulation and data analysis. The effective approach presented in this paper for generator fault diagnosis using the acquired SCADA data shows the importance of simulation models in providing guidance for post-data analysis and interpretation. WT generator winding lifetime is finally estimated based on a thermal ageing model to investigate the impacts of wind speed and failure mode.

Keywords: wind turbine; generator; lumped parameter network; thermal analysis; ageing; fault detection and diagnosis

1. Introduction

While wind energy development shifting from onshore to offshore, the external environment in which wind turbines (WTs) are installed has become more and more harsh [1]. Once WT components are exposed in such environments and operate in varying wind for years, it is a big challenge to achieve predictable remaining lifetime, availability and maintainability. The doubly-fed induction generator (DFIG) is one of the mainstream configurations in the wind industry, having advantages such as low cost and complexity, requiring a low converter capacity, and decoupling of active and reactive power control [2]. Temperature is one of the key parameters to define component design and materials of DFIGs [3]. A survey on wind power plants showed the major root causes for generator downtime are windings, brushes and other electrical components. The generator and electrical system cause 23.2% of WT downtime, in comparison to the gears causing 19.4% downtime [4]. Since performance and efficiency of a generator depends on the thermal condition of its windings, understanding the power losses and the thermal mechanism within a DFIG are of great importance to the industry.

In the power generation process, power losses are dissipated as heat, which directly influences the efficiency of the generator, and the temperature rise due to heat dissipation will further lower the power generator efficiency. In addition, the temperature rise within a generator will accelerate the insulation ageing and therefore affect the life of the generator. The losses related to generator include copper losses, iron losses, mechanical losses and stray losses, which are illustrated in Figure 1 [5]. Internal losses and thermal analysis within the electrical generator is necessary both for proper ventilation design and generator optimization. Copper losses and iron losses are the basic losses for a DFIG stator under normal operation conditions. The stator loss is proportional to the square of the stator current. As for most induction generators, the iron loss is less than the copper loss and it also will not be affected by the load, therefore the iron loss is neglected in many studies [6].

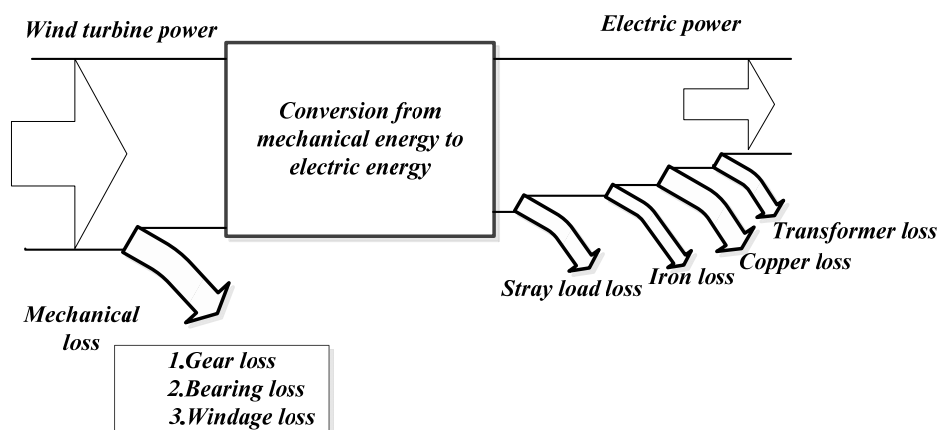


Figure 1. WT system power flow.

For a DFIG, the most important convection heat transfer occurs between the stator and air gap, and also between the stator windings and cooling fluid [7]. Additionally, an inner fan is installed on the shaft so as to transfer the heat to the external environment. The process is illustrated in Figure 2 where the arrows represent the air flow situation.

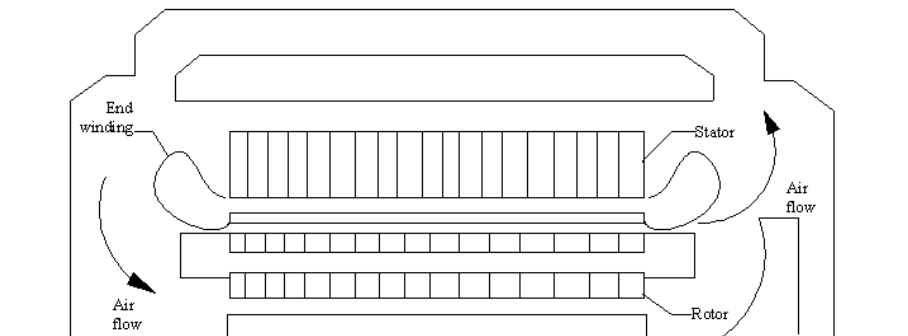


Figure 2. Sketch of the inner construction of a DFIG.

Thermal analysis of a generator is a complex problem where a number of heat exchanges are involved. Conduction, natural and forced convection and radiation are all present, and are affected by machinery electrical performance and its specific ventilation system design (natural cooling, fan cooling and water cooling, *etc.*). A coupled thermal-electromagnetic analysis approach was used to accurately predict induction motor performance. For thermal analysis, the two main approaches are analytical Lumped Parameters Network (LPN) and numerical methods. The application of these analytical techniques depends on the specific machine under study and requires considerable tailoring and modification for purpose. Commercial software packages using numerical methods based on Finite Element Analysis (FEA) or Computational Fluid Dynamics (CFD) can perform complicated multi-dimensional simulations, but they are normally time-consuming and the parameters are often difficult to determine. LPN or equivalent thermal network methods simplify the heat transfer mechanism into a thermal network with lumped parameters. The main advantages of the LPN method, such as low computational cost and capability to include the heat transfer of the cooling system, make it an appropriate method for thermal analysis of radial flux electrical generators [8].

The thermal network model has been used for transient and steady state temperature analysis of an asynchronous generator [8]. A real-time thermal model is shown for a Permanent Magnet Synchronous Motor (PMSM) which state-space format was discretized, and a model-order reduction was applied to minimize the complexity [9]. Although the LPN method has been successfully applied in induction generator thermal analysis, the aforementioned studies mostly focus on the thermophysics of generators and make the assumption of constant output torque and rotating speed. In fact, wind speed variation and control system have impacts on the thermodynamics of a WT generator. By taking into account the thermal characteristics under variable-speed operating conditions, thermal analyses should be performed to ensure the machine meets its design requirements.

Generator winding failures due to stator insulation breakdown are known as one of the most serious causes of failure. Stator insulation is affected by thermal, electrical, and mechanical stresses, as well as environmental conditions. Temporarily increasing high winding temperatures, e.g., caused by a

ventilation system failure, can lead to permanent changes of the properties of the insulation system and even asphaltic run [10]. In these cases the lifetime can be reduced significantly and diagnostic tests should be performed to estimate the remaining life.

In this paper, a DFIG thermal model is firstly incorporated in a variable-speed WT model to study the thermodynamics of generator stator winding. The transient-state and steady-state temperature characteristics of stator winding under different wind speed patterns are studied. Then, applications of thermal analysis of WT DFIG on fault detection and diagnosis, and generator insulation lifetime estimation are presented. By combining both simulation and realistic data analysis, the thermal mechanisms of two failure modes, *i.e.*, generator ventilation system failure and supply voltage unbalance, are analyzed in detail to interpret the acquired data.

2. Methodology

The methodology of electro-thermal analysis of DFIG in a WT is shown in Figure 3. An electrical model is developed based on principle analysis of a wind turbine with DFIG configuration which considers the corresponding control strategy. Failure modes are then introduced into the electrical model to derive the variations of electrical parameters under fault conditions. A power loss mechanism is analyzed for the thermal model. The intrinsic thermal process of the DFIG is analyzed by an LPN model which is actually coupled to the thermal model. The variation of thermal parameters such as temperature rises of different failure modes are quantified by this electro-thermal method for fault diagnosis and thermal ageing prediction.

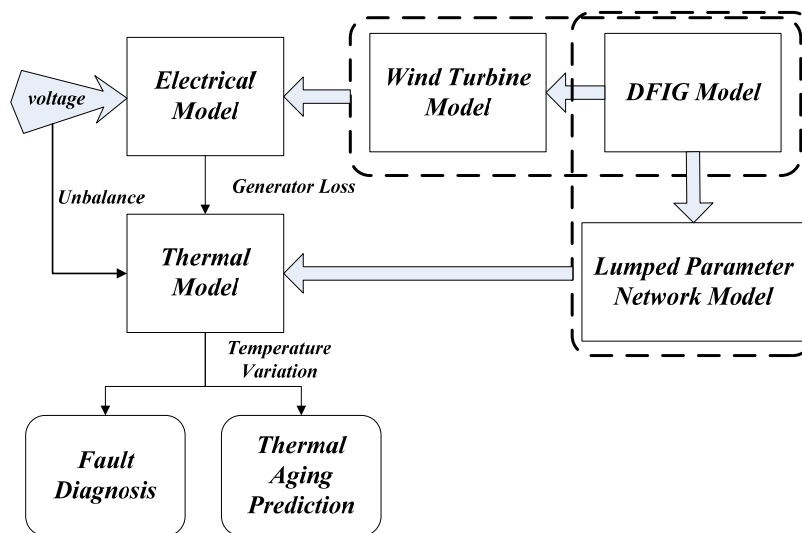


Figure 3. The methodology of an electrothermal analysis for DFIG in WT.

2.1. Wind Turbine Model

Figure 4 shows a WT with DFIG configuration. It is composed of blade, rotor, pitch system, gearbox, generator and controller. All these subsystems are controlled to realize the procedure of converting mechanical energy into electricity. The auxiliary systems in a WT include the cooling, lubrication and protection systems [11].

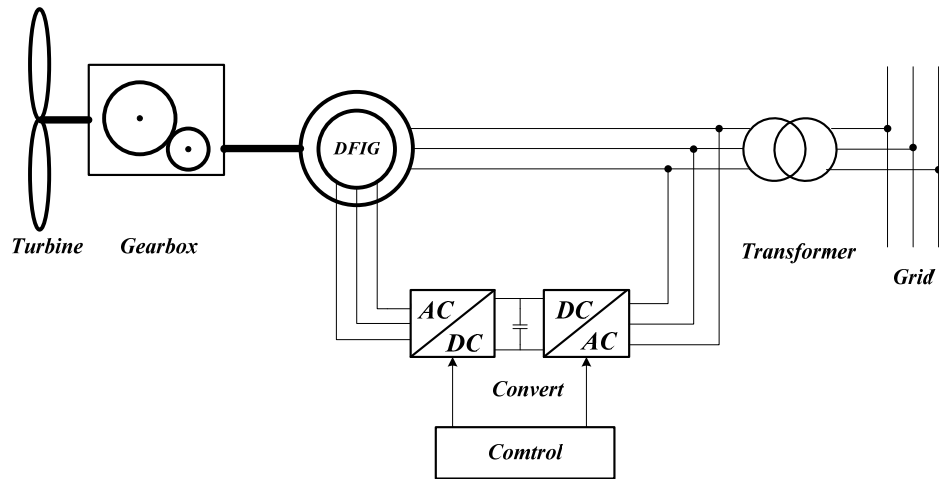


Figure 4. Configuration of a WT with DFIG.

(1) Aerodynamic principle

According to Betz theory, the power P extracted from the wind can be expressed by Equations (1)–(3) shown below:

$$P = \frac{1}{2} C_p(\lambda, \beta) \rho \pi R^2 v^3 \quad (1)$$

$$\lambda = \frac{\omega R}{v} \quad (2)$$

$$T = \frac{P}{\omega} = \frac{1}{2} C_p(\lambda, \beta) \rho \pi R^2 \frac{v^3}{\omega} \quad (3)$$

where ρ is the air density (kg/m^3), P is the derived power of WT (W), C_p is the power coefficient, λ is the tip speed ratio, β is pitch angle (rad), R is the radius of WT (m), v is the wind speed (m/s), ω is the rotor speed (rad/s), T is the rotor torque of WT ($\text{N}\cdot\text{m}$).

(2) Drive train model

$$(J_r + J_g \frac{n^2}{\eta}) \frac{d\omega_r}{dt} = T_r(\omega_r, v) - \frac{n}{\eta} T_g(\omega_g, c) \quad (4)$$

Assuming a rigid drive train model, J_r is the rotational inertia of the WT rotor ($\text{kg}\cdot\text{m}^2$), J_g is the rotational inertia of the generator rotors, ($\text{kg}\cdot\text{m}^2$), T_r is the aerodynamic torque of the WT ($\text{N}\cdot\text{m}$); T_g is the mechanical torque of the high-speed shaft ($\text{N}\cdot\text{m}$) which is connected to the generator, ω_r is the rotor speed (rad/s), ω_g is the generator speed (rad/s), n is the transmission ratio of gear box, η is the efficiency of the gearbox.

2.2. Control Strategy

For a WT with DFIG, a Maximum Power Point Tracking (MPPT) control strategy is implemented in the range of wind speeds below the rated maximum by controlling the electromagnetic torque of the

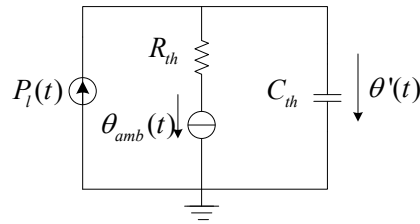


Figure 6. A generic thermal network model of the stator windings.

$P_{loss}(t)$ is the heat source determined by the stator winding power loss in the DFIG, which magnitude is determined jointly by the stator winding resistance and the current passing through:

$$P_{loss}(t) = I^2 R \quad (5)$$

I and R are the current and resistance of the generator stator winding, respectively. To consider the temperature effects to stator winding resistance, Equation (6) is used as follows:

$$R = R'(1 + \alpha \Delta T) \quad (6)$$

where R' is the initial resistance of stator winding and R is its ultimate resistance with ΔT temperature variation. α is temperature coefficient of stator winding resistance.

In the LPN model, R_{th} is the thermal resistance; C_{th} is the thermal capacitance and $\theta_{amb}(t)$ is the ambient temperature which represents the environmental variation, and $\theta'(t)$ is the generator winding temperature. Thermal resistance R_{th} is determined jointly by the thermal conduction, convection and radiation resistances. With the equivalent thermal network model established above, the thermodynamics of the stator winding are derived as follows:

$$C_{th} \frac{d\theta'(t)}{dt} + \frac{\theta'(t)}{R_{th}} = P_{loss}(t) \quad (7)$$

The transfer function is:

$$G(s) = \frac{\theta(s)}{P_{loss}(s)} = \frac{R_{th}}{1 + \tau_{th} s} \quad (8)$$

where $\tau_{th} = R_{th}C_{th}$ is derived from Equation (8). The simplified thermal model is essentially a low-pass filter with a cut-off frequency of $\omega_c = 1/\tau_{th}$. The thermal resistance to model the convective heat transfer between the solid component and the fluid flow is $R_{th} = 1/(Ah)$. Failure of the ventilation system leads to the change of the heat transfer property, which is ultimately presented as a variation of the thermal parameters.

2.4. Thermal Ageing of DFIG Winding

This paper studies the reduction of stator winding insulation lifetime due to thermal stress. That is, the insulation ageing process will depend on the magnitude and duration of the operating temperature. Although thermal fatigue process is ignored in this paper, thermal ageing model is used to estimate the life of a generator with temperature fluctuation. According to the Arrhenius equation [13], the lifetime of insulation at elevated temperatures is expressed as follows:

$$\ln L = \ln B + \frac{\varphi}{kT} \quad (9)$$

where L is the life in units of time (min or hr), B is a constant, usually determined experimentally, φ is the activation energy (eV), T is the absolute temperature (K) and $k = 0.8617 \times 10^{-4}$ (eV/K) is the Boltzmann constant.

The thermal ageing model above can be modified by introducing the Half Interval Index (HIC) as insulation life is halved for every 10 °C rise in temperature. It can be written as Equation (10). This model allows estimating the insulation life for all insulation classes according to their HIC :

$$L_x = L_{100} \times 2 \exp\left[\frac{T_c - T_x}{HIC}\right] \quad (10)$$

where L_x is the lifetime percent at temperature (h), L_{100} is the lifetime percent at rated temperature (h), T_x is the hot-spot temperature for insulation class (°C), T_c is the total allowable temperature for the particular insulation class (°C), HIC is the halving interval index. For winding insulation classes A, B, F, H and H', the corresponding HIC values are 14, 11, 9.3, 8, and 10. The insulation class limit is chosen as a 20,000 h (2.3 years) period in this paper. That is, the insulation is expected to operate continuously at its maximum temperature for 2.3 years without failing.

3. Results

3.1. Thermodynamics of DFIGs in Wind Turbines

The simulation performed in this paper is based on an onshore WT equipped with a DFIG. The DFIG has two poles pairs and is air cooled. The parameters used in the simulation are listed in Table 1.

Table 1. Wind turbine parameters.

Wind Turbine	Parameter	Generator	Parameter
Rated power	850 kW	Rated voltage	690 V
Rotor radius	25 m	Frequency	50 Hz
Rated wind speed	12 m/s	Stator resistance	0.016 Ω
$C_{p_{max}}$	0.436	Stator inductance	6.854 mH
λ_{opt}	8	Moment of inertia	30 Kg·m ²
Air density	1.225 kg/m ³	Pole pairs	2

To obtain the generator temperature variation curve, $R_{th} = 1/25\text{K/W}$, $C_{th} = 4,000 \text{Ws/K}$, ambient temperature $\theta_{amb}(t) = 20 \text{ °C}$ are assumed in the model [14]. The initial winding temperature is set as 0 °C and the simulation period is for 1,400 s. With the parameters above, the normalized power curve of the model WT is shown in Figure 7a. The normalized power loss and absolute stator winding temperature are obtained, and plotted against wind speed (Figure 7b,c). Power losses of the generator and the temperature of stator winding increase with wind speed.

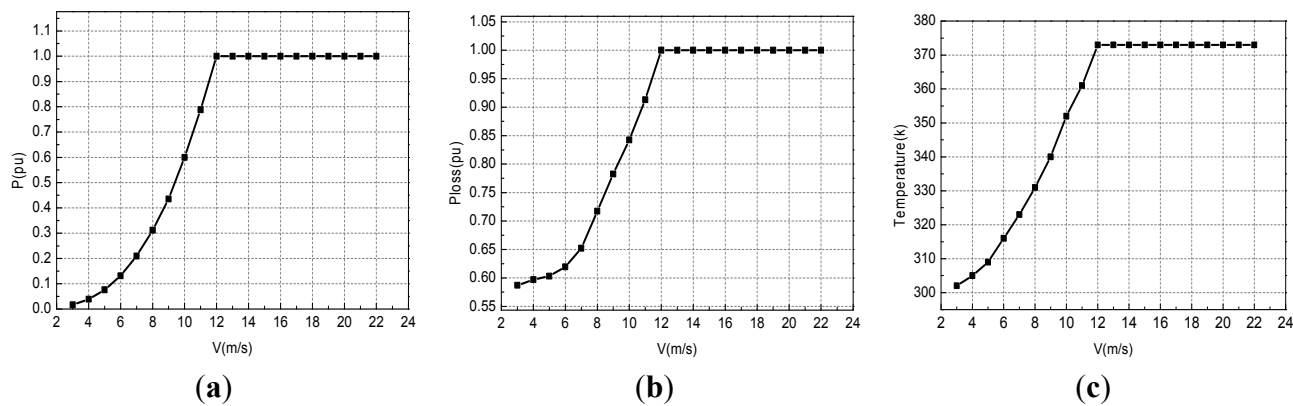


Figure 7. Power curve (a); Power loss against wind speed (b); Absolute stator winding temperature vs. wind speed (c).

The thermal behavior of the DFIG stator windings under constant wind speeds of 3, 7 and 12 m/s are obtained for a time period of 1,400 s, and shown in Figure 8. In the whole process, the generator ventilation system keeps operating continuously. From the moment that generator starts up, the stator winding experiences the first process of the machine approaching a stable operating condition and the winding reaching a constant temperature, then a second cooling down process after the machine stops at 600 s. At the higher wind speed, e.g., 12 m/s, the stable temperature reaches a higher value around 370 K due to the increase of output power. Although the thermal parameters R_{th} & C_{th} determine the time when the stator winding reaches a stable temperature, the wind speed will determine the reachable maximal temperature.

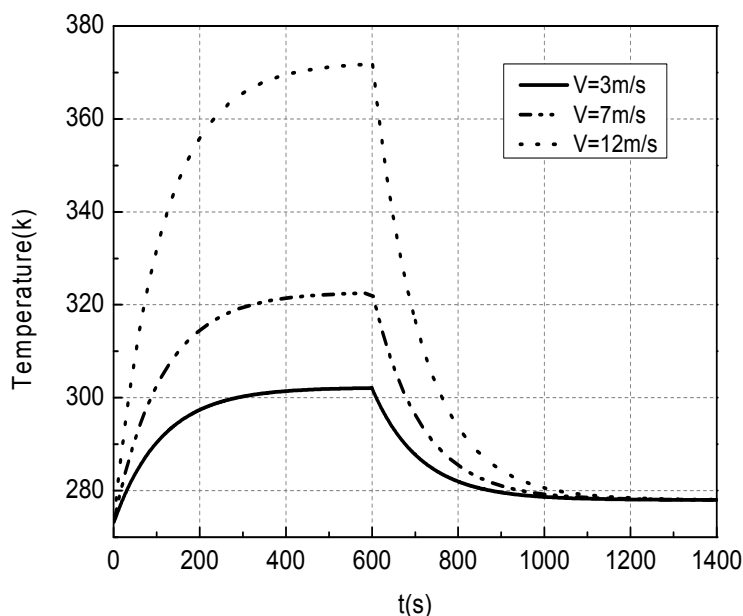


Figure 8. Thermal behaviour of the DFIG stator winding.

The mechanical, electrical and thermal responses of the DFIG under cyclic wind speed patterns are shown in Figure 9. A sudden rise of wind speed causes sharp increase of power losses, due to the transient current response in the stator winding, as shown in Figure 9d,e. However, the thermal response is not as fast as the electrical response as shown in Figure 9f. This is different from Figure 8, which shows that

the stator winding temperature rise is subject to thermal inertia *i.e.*, the temperature of the stator winding takes around 600 s or 10 min to reach its maximum. This is because when the wind speed changes in a step cycle between 3 m/s (*i.e.*, start-up) and 12 m/s (*i.e.*, full power) in just 20 s, as shown in Figure 9a, before the temperature of the stator winding reaches its stabilized value, the wind speed changes cause the temperature to vary, therefore, the temperature rise in the stator winding is between 4 K to 8 K (or °C) above the ambient temperature (*i.e.*, 20 °C or 293 K) as shown in Figure 9f.

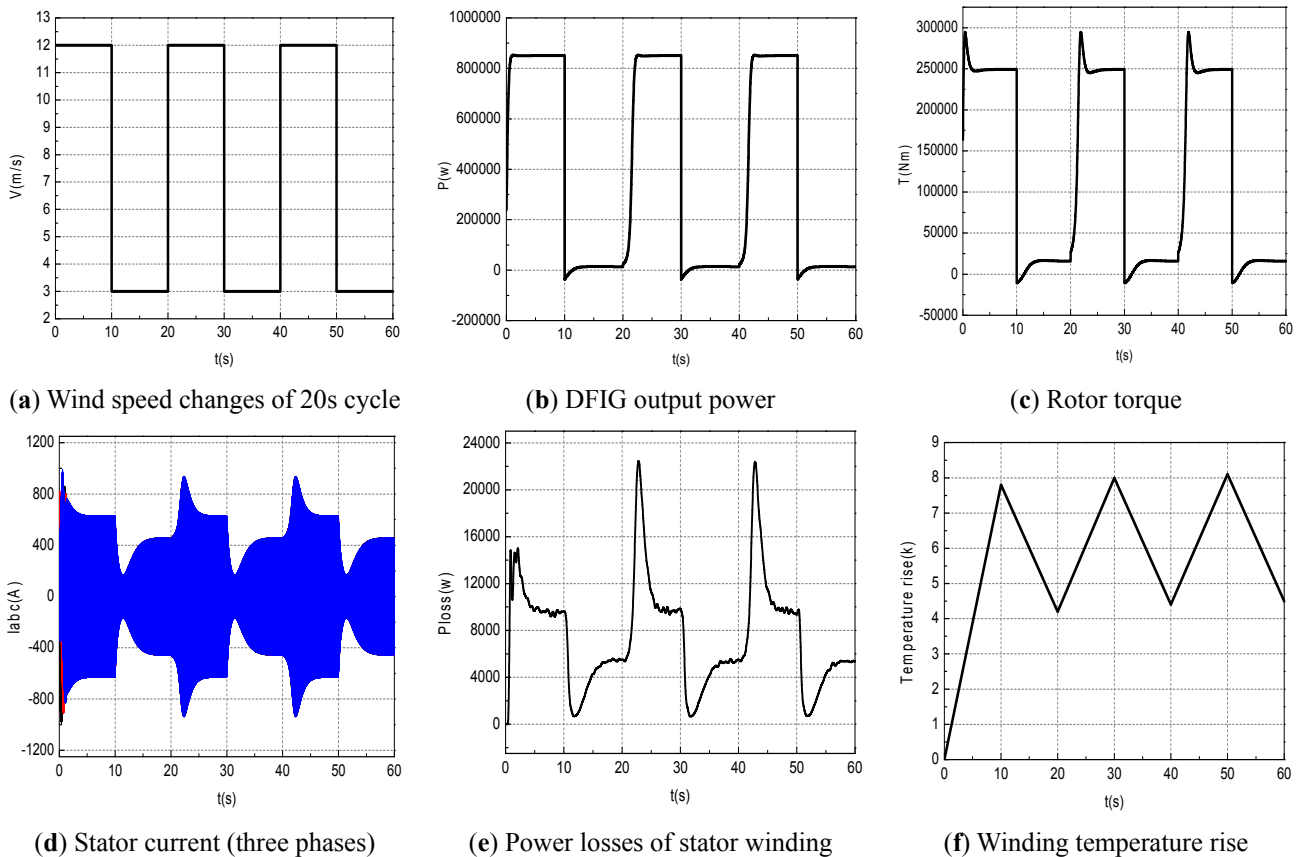


Figure 9. Mechanical, electrical and thermodynamics of the WT and DFIG stator winding under step-cycle wind speed conditions.

When the wind speed changes in a step cycles between 3 m/s (*i.e.*, start-up) and 12 m/s (*i.e.*, full power) in 30 s cycles (Figure 10) or in 40 s cycles (Figure 11), their power losses are the same but the temperature rises in the stator winding are quite different. In the 30 s case, Figure 10 shows the temperature rise is between 5 K to 10 K (or °C); In the 40 s case, Figure 11 shows the temperature rise is between 10 K to 18 K (or °C). For the same thermal parameters R_{th} & C_{th} , a DFIG machine operating with a longer high wind speed duration will experience a higher temperature rise. If the scale of the wind speed change is less than the above cases, e.g., between 3 m/s and 7 m/s, the magnitude of the temperature rise will be less. Therefore, the magnitude of temperature rise depends not only on the thermal parameters of the DFIG stator winding, but also on the wind speed profile, including the scale and cycle of the wind speed change.

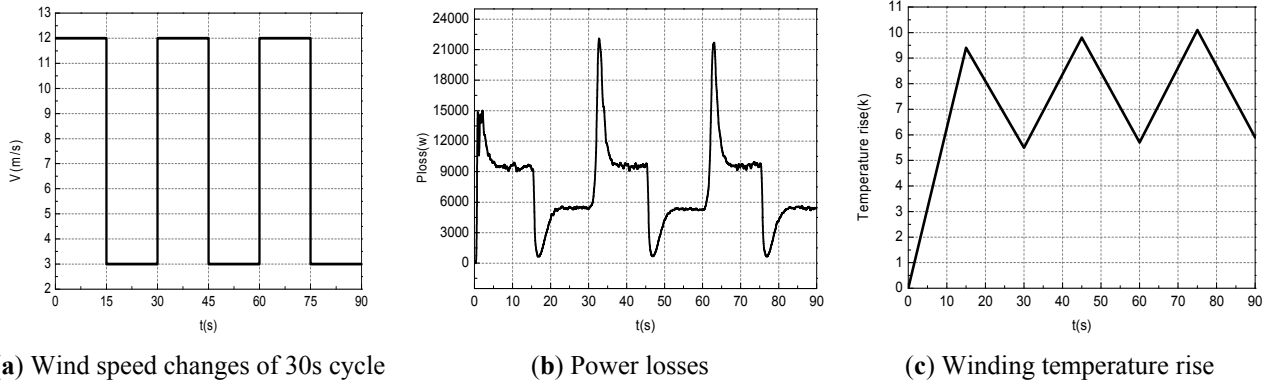


Figure 10. Power losses and temperature rise of stator windings for wind speed change with a 30 s cycle.

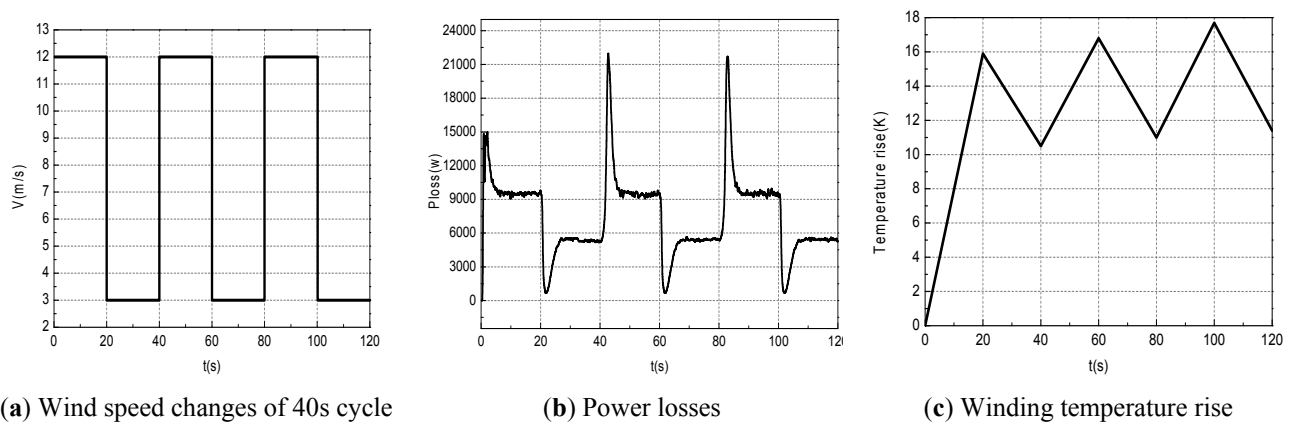


Figure 11. Power losses and temperature rise of stator windings a for wind speed change with a 40 s cycle.

3.2. Generator Case Studies: Voltage Unbalance vs. Ventilation Fault

Voltage unbalance, also known as the phase voltage unbalance rate (PVUR), is defined as below according to the IEEE definition:

$$PVUR = \frac{Max .voltage deviation from Avg .phase voltage magnitude}{Avg .phase voltage magnitude} \times 100 \tag{9}$$

Even with the same voltage unbalance factor [15], there could be a single phase, two-phase or three-phase voltage unbalance. Here a three-phase voltage unbalance with 10% PVUR and a two-phase unbalance with 5% PVUR (b & c phases) are injected in the DFIG model to examine the corresponding thermal behaviors. The results are shown in Figure 12.

Figure 12a shows a case of 10% PVUR variation for the whole three-phase voltage on a time scale. The generator operates at the rated voltage for the first 200 s, then a 10% overvoltage for the next 200 s, and finally 10% under-voltage for the remaining 200 s. Figure 12b shows the corresponding stator winding temperature changes. Figure 12c shows the stator currents under two-phase (b & c) voltage unbalance with 5% PVUR injected at 300 s. Figure 12d shows a, b & c stator winding temperature changes. During voltage unbalance, the three-phase currents of the DFIG are non-uniform. It is quite clear that the temperature of the windings changes subject to different voltage unbalance situations.

There are several causes leading to voltage unbalance such as incomplete transposition of transmission lines, unbalanced loads, open delta transformer connections, blown fuses on three-phase capacitor banks. Apart from the grid code violation, the voltage unbalance will also have negative impacts on electric machines, such as overheating, current unbalance, de-rating and inefficiency, leading to winding insulation degradation [16].

For a wind turbine with DFIG configuration, MPPT control is realized under the rated wind speed range to tune the rotor speed through electromagnetic torque control of the induction generator. As the induction generator torque is subject to the rotor current and stator voltage, therefore any unbalance of the stator voltage will cause an unstable rotor current in order to maintain an appropriate torque value rather than to maintain a constant power output. Therefore, an increase of stator voltage will cause a slight increase of stator current, and thus an increase of winding temperature.

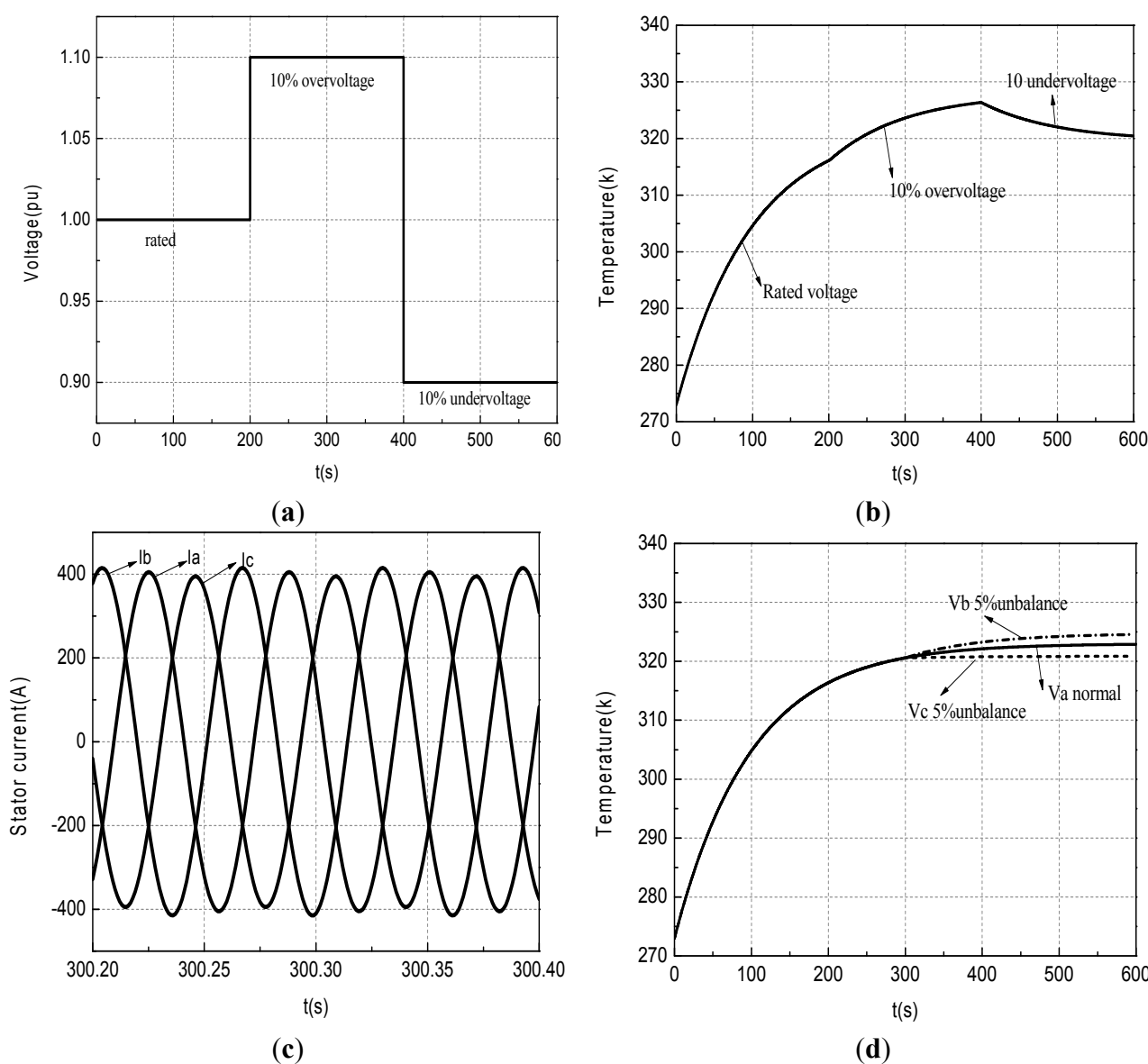


Figure 12. DFIG stator winding temperature variation due to different PVUR situations. (a) Three-phase voltage unbalance; (b) Temperature for three-phase unbalance; (c) b & c phase voltage unbalance; (d) Temperature for two-phase unbalance.

3.3. Comparisons between Simulation Results and Real WT Data

Performance data such as temperature and power output are continuously monitored by the WT SCADA system. Here real data are collected in a 10-minute interval from an operating 1–2 MW WT, and further averaged in block according to the normalized power output. The temperatures of the generator stator windings are measured by PT100 thermal resistance elements which are embedded in the windings. To reduce the data volume, the SCADA system recorded the average temperature measured from the PT100s installed in different locations of the generator stator winding. Figure 13 shows the real data collected under two conditions by plotting the absolute winding temperature rise (K) vs. normalized power output (pu) for a DFIG operating under healthy conditions (circles), and after generator ventilation failure (squares). The simulated data are further plotted under the same conditions: DFIG operating under healthy conditions (solid line), and after generator ventilation failure (dashed line). Besides the generator rating, the parameters in the simulation model such as stator winding resistance, thermal resistance and capacitance in the LPN model are adjusted accordingly to match the real data. The stator winding resistance is set to 0.016Ω and its temperature coefficient is chosen as $0.0039 \Omega/K$. It is clear in Figure 13 that good agreement between the simulation result and the real data is reached. From the simulation, the R_{th} is 0.0101 K/W and C_{th} is $19,200 \text{ Ws/K}$ before the generator ventilation failure, however, R_{th} increases to 0.0174 K/W and C_{th} remains the same after the ventilation failure. When the ventilation system is faulty, an increase of the gradient and the same intercept are found in the plot of stator winding temperature rise against power output.

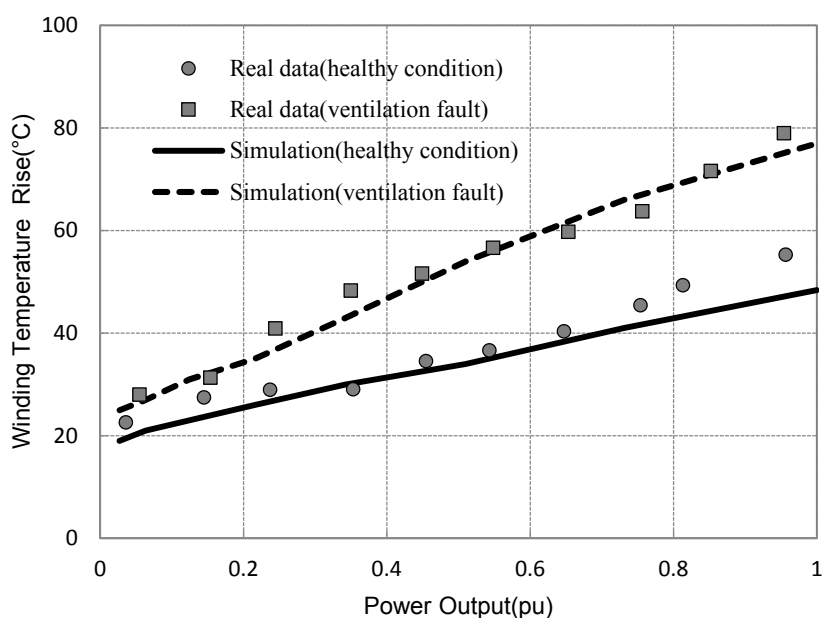


Figure 13. Winding temperature rise against normalized power output when DFIG under healthy condition and with ventilation system fault.

It is important to understand the thermal process within a DFIG generator with a faulty ventilation system. Since the generator is air-cooled, the air flow inside the generator will change from forced convection to natural convection as long as the ventilation system is faulty. In this situation, it is more difficult to dissipate the heat, which leads to an increase of the convection resistance coefficient. Due to

the increase of the internal temperature of the DFIG, the stator winding resistance will increase with the temperature coefficient of $0.0039 \text{ } \Omega/\text{K}$ of copper. This further leads to an increase of power loss. The increase of power loss and the variation of thermal resistance will lead to an increase of the winding temperature rise. The fitting shows that a good agreement is obtained by increasing the thermal resistance from 0.0101 K/W to 0.0174 K/W for the DFIG switching from healthy situation to faulty ventilation circumstances. The temperature rise of the DFIG is determined jointly by the stator winding resistance and thermal resistance while the thermal capacity C_{th} remains the same. The increase of thermal resistance of R_{th} will also result in a shorter time for the generator temperature to become stable, which can be observed from the detailed analysis that shows increased scattering of the temperature data

Figure 14 shows the real data of absolute winding temperature rise (K) vs. normalized power output (pu) collected under another two conditions: a DFIG operating under healthy conditions (circles), and a DFIG operating under all three-phase voltage unbalance with 5% overvoltage (triangles). Similarly, the simulated data are further plotted under the same machine conditions, including a DFIG operating under healthy conditions (solid line) and a DFIG operating with a three-phase voltage unbalance with 5% overvoltage (dotted line). After the supply voltage is unbalanced with 5% overvoltage, the line intercept becomes greater, the gradient of stator winding temperature rise against power output remains the same as under healthy conditions.

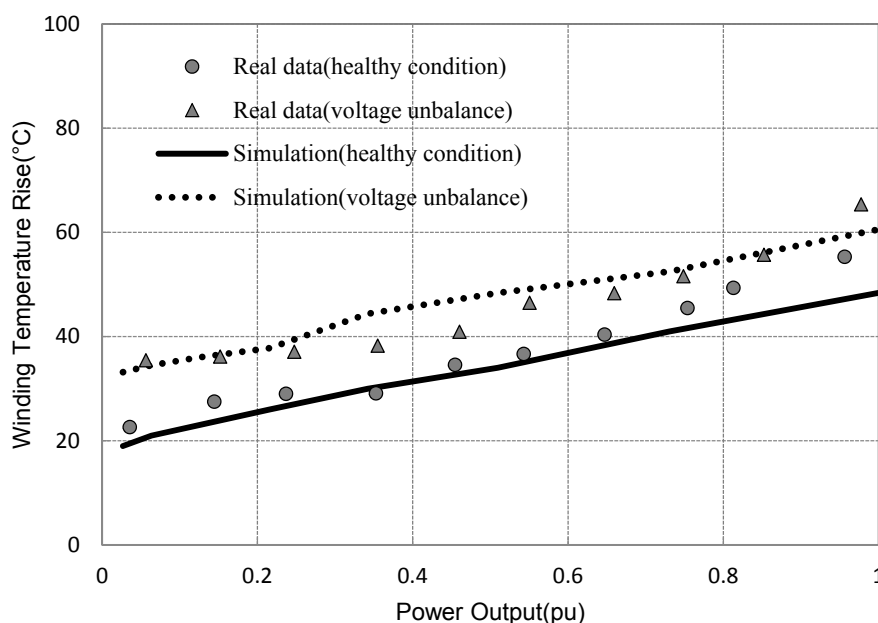


Figure 14. Winding temperature rise against normalized power output when the DFIG is under healthy conditions and with voltage unbalance.

The thermal mechanism due to voltage unbalance within the generator is different from a ventilation system failure. Voltage unbalance will have a direct impact on the generator output current, which further affects the losses in the generator. In this case, both the current and resistance of the stator winding increases while the thermal resistance and capacity is the same as the healthy situation. The result shows that a 5% overvoltage on the DFIG leads to a 6–12 K (or °C) temperature increase in the generator stator winding. The magnitudes of the temperature increases are nearly in proportion for different power

generations. It is proved by the same gradient as shown in the plot. By combining both simulation and real data analysis, a curve of winding temperature against power output can reveal certain thermals mechanism in the DFIG. Failure modes related to the change of thermal behaviors such as ventilation faults and voltage unbalance can be distinguished clearly using this approach. The approach is thus proven to be useful for fault detection and diagnosis of WT DFIGs and the simulation model plays a key role in providing guidance for post-data analysis and interpretation.

3.4. Influence of Wind Speed and Failure Mode on Winding Lifetime

Assuming Class F insulation for a generator stator winding, Figure 15a shows the estimated lifetime of a WT DFIG operating at a certain wind speed. Under healthy operating conditions, the estimated lifetime of the DFIG will be reduced by an increase of wind speed. Figure 15a also shows the estimated lifetime of stator windings subjected to two failure modes, *i.e.*, voltage unbalance with 10% overvoltage and ventilation system failure with thermal resistance increasing by 12.5% and thermal capacitance decreasing by 46.2%. In the higher wind speed range above 7 m/s, ventilation failure has a greater impact on shortening generator lifetime. However, the voltage unbalance has nearly the same effects on shortening generator lifetime at different wind speeds, so the estimated lifetime curve is shifting downwards vertically. Figure 15b shows the estimated lifetimes of stator windings with different Class ratings. To choose an appropriate generator insulation Class, a tradeoff should be made between lifetime and overall cost.

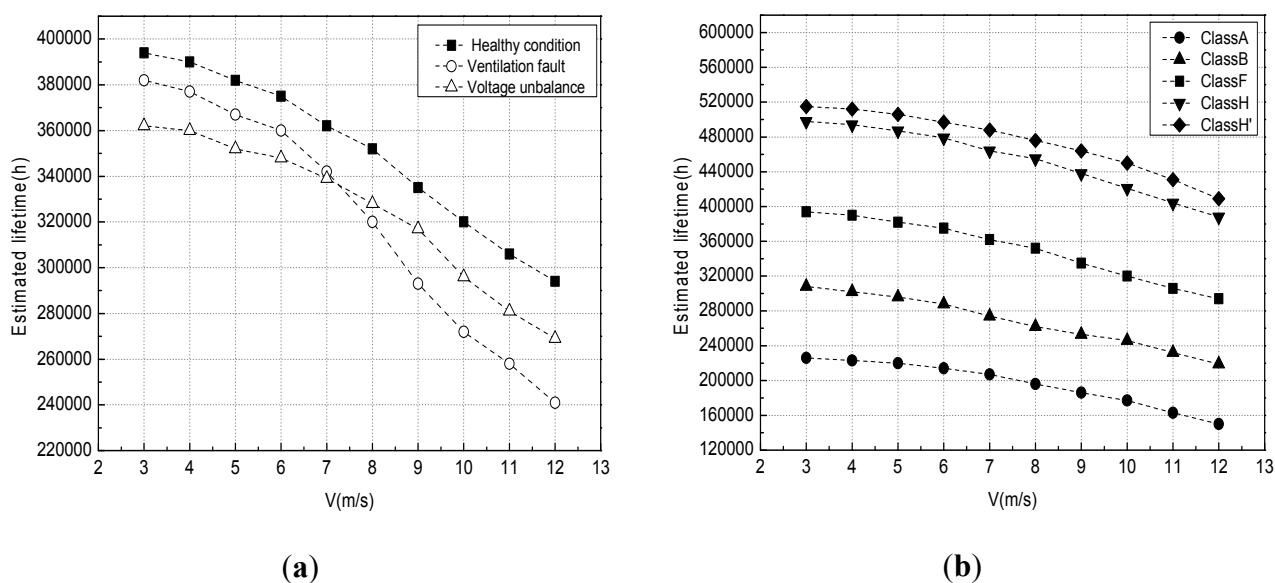


Figure 15. Lifetime downrating of stator windings subjected to generator system faults (a); lifetime estimation of stator windings with different Class ratings (b).

4. Conclusions

The paper developed an electro-thermal model for the DFIG in a WT. The generator power loss mechanism is analyzed and a simplified thermal network model is formed using lumped circuit parameters. Then it is incorporated into a WT system model to study the influence of wind speed on the steady and transient thermal behaviors of DFIG stator windings. The conclusions are as follows:

- (1) The thermal mechanism within the WT generator is different from that of conventional machines with constant rotational speed, *i.e.*, the power losses within a WT generator are mostly affected by the wind speed profile, which further determines the magnitude of the stator winding temperature.
- (2) While the long-term/steady state temperature characteristics of WT generator are determined by the power loss mechanism, the short-term/transient characteristics are determined by the thermal parameters, *i.e.*, the thermal resistance and capacitance reflect the thermal process within the generator.
- (3) A generator ventilation failure will cause an increase of winding resistance, and thermal resistance of the LPN model. This essentially reflects an interaction effect between power losses and the thermal process of the ventilation system within a generator.
- (4) Supply voltage unbalances will cause an increase of generator output currents and an increasing magnitude of power losses within the generator. In this process, the electro-thermal effects dominate and thermal parameters remain the same.
- (5) In the curve of stator winding temperature rise against power output, depending on the specific failure mode, the gradient and intercept of the curve will be different. Simulation clearly demonstrates the physical meanings corresponding to the curve changes, based on which effective fault detection and diagnosis can be easily implemented and interpreted.
- (6) Both wind speed and failure mode have negative impacts on generator lifetime. At high wind speed, ventilation system failures will cause more damage to the generator.

Acknowledgments

This is a research work funded by The Natural Science Foundation of Jiangsu Province (BK2013135), Start-up Scientific Research Project of NUST, Jiangsu Top Six Talent Summit Fund (ZBZZ-045). Returned Overseas Students Preferred Funding. The Fundamental Research Funds for the Central Universities, No. 30915011324.

Author Contributions

All the authors contributed equally to the theoretical model development, data analysis and interpretation of the comparison results.

Conflicts of Interest

The authors declare no conflict of interest.

References

1. Perveen, R.; Kishor, N.; Mohanty, S.R. Off-shore wind farm development: Present status and challenges. *Renew. Sust. Energ. Rev.* **2014**, *29*, 780–792.
2. Liserre, M.; Cardenas, R.; Molinas, M.; Rodriguez, J. Overview of Multi-MW wind turbines and wind parks. *IEEE Trans. Ind. Electron.* **2011**, *58*, 1081–1095.

3. Nienhaus, K.; Hilbert, M.; Baltes, R.; Bernet, C. Statistical and time domain signal analysis of the thermal behavior of wind turbine drive train components under dynamic operation conditions. *JPCS* **2012**, *364*, 012132.
4. Ribrant, J.; Bertling, L. Survey of failures in wind power systems with focus on Swedish wind power plants during 1997–2005. *Trans. Energy Conversion* **2007**, *22*, 167–173.
5. Inoue, A.; Takaahashi, R.; Murata, T.; Tamura, J.; Kimura, M.; Futami, M. A calculation method of the total efficiency of wind generators. *Electr. Eng. Jpn.* **2006**, *157*, 52–62.
6. Stone, G.; Boulter, E.A.; Culbert, I.; Dhirani, H. *Electrical Insulation for Rotating Machines—Design, Evaluation, Aging, Testing, and Repair*; Wiley-Interscience: Hoboken, NJ, USA, 2004; pp. 137–179.
7. Alberti, L.; Bianchi, N. A Coupled thermal–electromagnetic analysis for a rapid and accurate prediction of IM performance. *IEEE Trans. Ind. Electron.* **2008**, *55*, 3575–3582.
8. Boglietti, A.; Cavagnino, A.; Staton, D.; Shanel, M.; Mueller, M.; Mejuto, C. Evolution and modern approaches for thermal analysis of electrical machines. *IEEE Trans. Ind. Electron.* **2009**, *56*, 871–882.
9. Demetriades, G.D.; De La Parra, H.Z.; Andersson, E.; Olsson, H. A real-time thermal model of a permanent-magnetic synchronous motor. *IEEE Trans. Power Electron.* **2010**, *25*, 463–474.
10. Oraee, H. A quantitative approach to estimate the life expectancy of motor insulation systems. *IEEE Trans. Dielectr. Electr. Insul.* **2000**, *7*, 790–796.
11. Takahashi, R.; Ichita, H.; Tamura, J. Efficiency calculation of wind turbine generation system with doubly-fed induction generator. In Proceedings of the 2010 XIX International Conference on Electrical Machines (ICEM), Rome, Italy, 6–8 September 2010.
12. Xu, L.; Wang, Y. Dynamic modeling and control of DFIG-Based wind turbines under unbalanced network conditions. *IEEE Trans. Power Syst.* **2007**, *22*, 314–323.
13. Brancato, E.L. Estimation of lifetime expectancies of motors. *IEEE Electr. Insul. Mag.* **1992**, *8*, 5–13.
14. Nienhaus, K.; Hilbert, M. Thermal analysis of a wind turbine generator by applying a model on real measurement data. In Proceedings of the 2012 IEEE International Workshop on Applied Measurements for Power Systems (AMPS), Aachen, Germany, 26–28 September 2012.
15. Siddique, A.; Yadava, G.S.; Singh, B. Effects of voltage unbalance on induction motors. In Proceedings of the 2004 IEEE International Symposium on Electrical Insulation, Indianapolis, IN, USA, 19–22 September 2004.
16. Pillay, P.; Manyage, M. Loss of life in induction machines operating with unbalanced supplies. *IEEE Trans. Energy Conversion* **2006**, *21*, 813–822.